Developmental Biology 425 (2017) 58–69

Contents lists available at ScienceDirect

Developmental Biology

journal homepage: www.elsevier.com/locate/developmentalbiology

Original research article

The activity of the *Drosophila* Vestigial protein is modified by Scalloped-dependent phosphorylation

Virginia L. Pimmett[a,1], Hua Deng[a,b,1], Julie A. Haskins[a], Rebecca J. Mercier[a], Paul LaPointe[a], Andrew J. Simmonds[a,*]

[a] Department of Cell Biology, Faculty of Medicine and Dentistry, University of Alberta, Edmonton, AB, Canada T6G2H7
[b] Howard Hughes Medical Institute, Dept. of Physiology, UT Southwestern Medical Center, 5323 Harry Hines Blvd, Dallas, TX 75390, USA

ARTICLE INFO

Keywords:
Drosophila
Vestigial
Vestigial-like
Scalloped
TEAD proteins
P38

ABSTRACT

The *Drosophila vestigial* gene is required for proliferation and differentiation of the adult wing and for differentiation of larval and adult muscle identity. Vestigial is part of a multi-protein transcription factor complex, which includes Scalloped, a TEAD-class DNA binding protein. Binding Scalloped is necessary for translocation of Vestigial into the nucleus. We show that Vestigial is extensively post-translationally modified and at least one of these modifications is required for proper function during development. We have shown that there is p38-dependent phosphorylation of Serine 215 in the carboxyl-terminal region of Vestigial. Phosphorylation of Serine 215 occurs in the nucleus and requires the presence of Scalloped. Comparison of a phosphomimetic and non-phosphorylatable mutant forms of Vestigial shows differences in the ability to rescue the wing and muscle phenotypes associated with a null *vestigial* allele.

1. Introduction

Development of adult tissues in *Drosophila* is a complex process relying on the activity of "selector" genes in specific cell sub-populations that define and/or maintain identity as they differentiate from precursor epithelial cells (reviewed in Hariharan (2015)). Selector genes most often encode transcriptional regulatory proteins that drive a specific program of gene expression that specify individual cell fates to form terminally differentiated structures. *vestigial* (*vg*) is a key selector gene involved in differentiation of the wing blade from the wing imaginal disc (Williams et al., 1991). *vg* is necessary for both proliferation and specification in the larval wing imaginal disc, as loss causes an absence of the entire adult wing, while ectopic expression drives trans-differentiation of non-wing ectodermal tissues into a wing fate (Kim et al., 1996; Simmonds et al., 1998; Williams et al., 1991).

In addition to the well-characterized role in the wing, Vg has been shown to be involved in differentiation of other tissues. In the developing embryonic mesoderm, Vg acts as a regulator of late-stage muscle differentiation. Loss of Vg causes a weakened embryonic muscle phenotype with diminished attachments and muscle loss in the ventral lateral muscles (Deng et al., 2009, 2010). Vg is also necessary for the formation of the indirect flight muscles, wherein Notch-dependent Vg signaling is required for proper muscle specification (Bernard et al., 2009). Loss of Vg via a vg^{null} allele causes apoptotic degradation of the muscle fibres resulting from transition to a direct flight muscle-like cell fate (Bernard et al., 2003, 2009).

Vg is the founding member of the Vestigial-like (*VGLL*) gene family. In *Drosophila*, there are two Vestigial-like genes, *vg* (Williams and Bell, 1988) and *tondu-domain-containing growth inhibitor* (*tgi*) (Koontz et al., 2013). *vg* is most closely related to the mouse and human *vestigial-like 1–3* (*VGLL1–3*) genes based on the presence of a single conserved TONDU domain, while *tgi* is orthologous to *VGLL4* in both mice and humans owing to the presence of paired TONDU domains that are also highly conserved (Koontz et al., 2013). In vertebrates, VGLL proteins are expressed in several tissues. VGLL1-3 are found in placenta, while VGLL2 alone is in skeletal muscle (Maeda et al., 2002). The muscle-specific role for *vg* orthologues is maintained in other vertebrate species as well. VGLL2 orthologues are expressed in similar tissues, with the *Danio rerio* orthologue VITO-2b expressing transiently in developing myocytes (Mann et al., 2007), VGL-2 in the chick myotome (Chen et al., 2004) and VGL-2 in the developing *Xenopus* skeletal musculature (Faucheux et al., 2010).

Vg requires protein partners to regulate transcription in both muscle and wing primordia (Deng et al., 2010; Faucheux et al., 2010; Paumard-Rigal et al., 1998; Pobbati and Hong, 2013). As Vg itself has no appreciable DNA-binding capability, it functions via interaction with Scalloped (Sd) (Simmonds et al., 1998). Sd has a TEA domain (TEAD) DNA binding motif and interacts with Vg via the conserved

* Corresponding author.
[1] These authors made equal contributions.

http://dx.doi.org/10.1016/j.ydbio.2017.03.013
Received 3 August 2016; Received in revised form 1 February 2017; Accepted 14 March 2017
Available online 18 March 2017
0012-1606/

TDU domain. This regulates the subcellular localization of Vg as well as directs binding to target genes (Campbell et al., 1992; Halder et al., 1998; Simmonds et al., 1998). Interactions between Vg and Sd cause a target switch to wing fate genes in the wing imaginal disc (Halder and Carroll, 2001). A Vg-Sd interaction is also necessary for the proper formation of embryonic somatic musculature (Deng et al., 2009, 2010). In addition to wing development, Vg also plays a conserved role in embryonic somatic muscle specification (Deng et al., 2010). Vg interacts in a non-obligate fashion with both Sd and the pan-muscle transcription factor Myocyte Enhancer Factor 2 (Mef2) to promote specification of the dorsal acute 1–3, lateral longitudinal-1, and ventral lateral (VL) 1–4 muscles (Deng et al., 2009). This mesodermal function is evolutionarily conserved, as the human Vestigial-like protein VGLL-2 is co-expressed alongside the Sd orthologue TEAD-1/TEF-1 in embryonic somites and branchial arches as well as adult skeletal muscle (Maeda et al., 2002).

Sd has other roles during wing specification independent of the interaction with Vg, including a role in the development of the anterior wing margin sensory bristles (Jack and DeLotto, 1992; Morcillo et al., 1996). In addition to the wing imaginal discs, Sd is also expressed in the embryonic nervous system, where it may be involved in neuromuscular pathfinding (Guss et al., 2013), as well as the embryonic heart (Deng et al., 2009) and the larval wing, haltere, leg and eye-antennal discs (Guss et al., 2013).

While TEAD homologues are present in single cell eukaryotes, VGLL proteins seem to be restricted to metazoans. In *Saccharomyces cerevisiae*, there is only a single Sd orthologue (TEC1; Laloux et al., 1990) and no Vg orthologue. Mice and humans have four Sd orthologues in the TEAD family (TEAD1-4; Zhao et al., 2010). Loss of TEAD proteins in mice leads to a range of phenotypes, from preimplantation lethality in a TEAD4$^{-/-}$ mouse (Yagi et al., 2007) to normal adult mice with no apparent defects in TEAD2$^{-/-}$ mutants (Sawada et al., 2008). These proteins are known to bind the VGLL family proteins across a range of species. However, TEAD family proteins have several other known binding partners, including the Hippo pathway effector Yes-associated protein (YAP; Wu et al., 2008; Zhang et al., 2008), Mask (Sidor et al., 2013) and Mef2 (Deng et al., 2009) that have both activating and repressing functions across multiple tissue types. In addition to acting as a partner for Vg, Sd also has a role in modulating gene regulation in the Hippo pathway through interacting with the transcriptional cofactor Yorkie (Yki). This interaction has been proposed to be modulated by the presence of Vg family proteins, as formation of Vg-Sd multimers may titrate available Sd in the cell and prevent an interaction with Yki (Koontz et al., 2013). Post-translational modifications to the Vg protein could help regulate Vg interaction with Sd or similar DNA binding proteins or directly affect Vg transactivation activity. Vg has previously been shown to be sumoylated (Takanaka and Courey, 2005), and this modification is necessary for activation of the Vg quadrant enhancer (QE) in S2 cells.

VGLL proteins have been identified as being involved in cancer progression (Alaggio et al., 2015; Jiao et al., 2014; Peng et al., 2014). All *VGLL* family members have been associated with cancer in humans. Suppressed expression of VGLL-4 in gastric cancer is associated with increased invasion and cell proliferation (N. Li et al., 2015), potentially by suppression of Wnt signaling (H. Li et al., 2015). This is strongly attenuated *in vitro* and *in vivo* by addition of a VGLL-4 peptide mimic, resulting in suppression of tumour growth through disruption of a YAP-TEAD interaction (Jiao et al., 2014). Loss of VGLL4 has also been associated with esophageal small cell carcinoma (Jiang et al., 2014) and lung adenocarcinoma (Zhang et al., 2014). Similarly, epithelial ovarian cancer (Gambaro et al., 2013) and prostate cancer (Peng et al., 2014) are both associated with diminished VGLL-3 expression, and VGLL-1 with a triple-negative/basal-like phenotype in breast cancer (Castilla et al., 2014). Infantile spindle cell rhabdomyosarcoma has been associated with chromosomal translocations leading to VGLL-2 fusion proteins (7 of 11 cases studied) as well as TEAD1 fusion proteins (3 of 11 cases; Alaggio et al., 2015). There is also a strong correlation between poor prognosis and expression changes of TEAD proteins and their coactivators, including the VGLL proteins (reviewed in Pobbati and Hong (2013). The interaction between VGLL and TEAD proteins is likely highly regulated in different cell types and increased knowledge of what regulates this interaction will give insight into how the interaction may influence disease progression in cancer, as well as implement fate decisions during development.

The repurposing of transcriptional regulators across multiple tissue contexts been repeatedly identified in *Drosophila*, including the repurposing of Vg in multiple tissue and regulatory contexts (Simon et al., , 2016). This makes *Drosophila* an excellent simplified model for probing genetic regulatory mechanisms of the *VGLL* gene family. In this study, we provide evidence that Vg activity in specific cell types is dependent on phosphorylation. Further we show that this phosphorylation of Vg is dependent on the presence of the partner Sd. Finally, this phosphorylation is functionally relevant *in vivo* to direct cell fate in both the developing wing imaginal disc and embryonic somatic musculature.

2. Methods and materials

2.1. Cell culture and transfections

Drosophila S2 cells were grown at 25 °C in SFX medium (Invitrogen, Carlsbad, CA) supplemented with 100U/ml penicillin and 100 μg/ml streptomycin (Invitrogen). Transfections were carried out using didecyldimethylammonium bromide (Han, 1996). For each experiment, 10^7 cells were transfected with 1 μg of the appropriate expression construct.

2.2. Drosophila strains

All crosses were done at 25 °C.The UAS-*HA-vg*, UAS-*HA-vg*^{S215A}, and UAS-*HA-vg*^{S215E} strains and their derivatives were made in our laboratory using P-element-mediated insertion. Multiple strains containing each transgene were established and lines matched for relative expression were determined by quantitative reverse-transcribed PCR (QRT-PCR). All other lines used in these experiments were obtained from Bloomington *Drosophila* Stock Centre (BDSC, Indiana).

2.3. Plasmids

The expression vectors for transfection of S2 cells were created using Gateway Technology (Invitrogen) and the *Drosophila* Gateway destination vectors (Terrence Murphy, Carnegie Institute of Washington, Baltimore, MD). The constructs containing the *vg::sd* fusion gene and *vgΔSID* have been described previously (Srivastava et al., 2002; Simmonds et al., 1998). An NLS sequence was added to the 5' end of *vg* gene by PCR using primers containing the NLS sequence from SV40 gene. Inverse PCR was performed using primers that amplify specific portions of the *vg* coding region shown in Fig. 4 to create Vg deletion expression constructs. Site-directed mutagenesis was performed to make point mutations in the *vg* coding region (QuickChange Site-Directed Mutagenesis Kit, Stratagene). The pNL3.1-VgQ reporter plasmid was constructed by PCR amplification of the Vestigial Quadrant enhancer (Guss et al., 2001) and insertion via Gibson cloning (New England Biosystems). The pGL4.54 plasmid was a gift from Dr. Francesca Di Cara.

2.4. Immunoprecipitation and immunoblotting

S2 cells were transfected with relevant expression constructs containing the HSP70 promoter or *act5c* promoter. For the HSP70 promoter, protein expression was induced by heating the cells in three by 30 min at 37 °C followed by a 30 min recovery after the first two

cycles and > 6 h after heat shock cycle 3. Cells were harvested, washed once in PBS with protease and phosphatase inhibitors (Roche), and resuspended in radio-IP (RIPA) buffer (50 mM Tris pH 8.0, 150 mM NaCl, 1.0% NP-40, 0.5% Deoxycholic acid, 0.1% SDS, and Complete protease inhibitor cocktail, Roche). The lysate was then incubated for 15 min at 4 °C with agitation, centrifuged for 15 min at 13.2 K rpm at 4 °C and supernatant transferred to a fresh tube. Co-IP reactions were carried out on 300 µl of supernatant (One half of a total of 600 µl supernatant from 25 cm^2 flask of cell culture) using 8 µl anti-FLAG M2-agarose beads (Sigma) in 500 µl RIPA buffer. Agarose beads were incubated for one hour at 4 °C with rocking, centrifuged for one min at 1.4 K rpm at 4 °C, and washed six times by vortexing in 500 µl RIPA buffer. Primary antibodies for immunoblotting were: mouse anti-FLAG (1:1000; Sigma), rat anti-HA (1:400; Roche), Rabbit anti-Vg (1:400; Williams et al., 1991), and rabbit anti-Myc (1:1000; Cell Signaling). Secondary antibodies were: goat anti-mouse Alexa680 or Alexa790 (1:5000; Invitrogen); goat anti-rabbit Alexa 680 or IRdye800 (1:5000; Invitrogen); goat anti-rat Alexa790 (1:5000; Invitrogen). Samples were separated on 1 mm low-bis-acrylamide (118:1) polyacrylamide gels, and transferred to nitrocellulose membranes that were scanned detected and analyzed using an Odyssey Infrared Imaging System (LI-COR).

2.5. 2D gel electrophoresis

S2 cells were transfected and heat shocked as described above, and flash frozen in liquid nitrogen for storage at −80C. The cell pellet was then resuspended in mild lysis buffer (20 mM HEPES pH 7.0, 50 mM NaCl, 1 mM EDTA, 0.5 mM EGTA, 1% Triton X-100) with Complete protease inhibitor (Sigma) and PhosStop (Sigma). Cells were lysed using a smooth Dounce and sheared with a 22 G needle, then incubated on ice for 10 min followed by pelleting of debris. Immunoprecipitation was performed using myc-Trap agarose beads (Chromotek) at 4 °C overnight, followed by washing with mild lysis buffer and division of the sample in two. One of the two half-samples was treated with lambda phosphatase (New England Biosystems) at 30 °C for 45 min. All samples were then resuspended in rehydration buffer with DTT. Isoelectric focusing was performed overnight on a Pharmacia IPGphor using an Immobiline DryStrip, pH4–pH7 (GE Healthcare) before loading onto a 10% polyacrylamide gel for second dimension resolution and transfer to nitrocellulose membrane. Membranes were probed with mouse anti-myc 9E10 (1:6000) and rabbit anti-Vestigial (1:1000; Williams et al., 1991), with secondary donkey anti-mouse Alexa790 and donkey anti-rabbit Alexa680 (both 1:5000; Abcam) antibodies. Scanning and intensity analysis was performed using the Odyssey Software (LI-COR) along with Excel (Microsoft) and Prism (Graphpad).

2.5.1. QRT-PCR

Twenty five wing disc pairs were isolated from third instar larvae of the indicated genotype. RNA was isolated by mechanical lysis followed by TRIzol purification of RNA (Life Technologies). RNA was reverse-transcribed using the iScript Select cDNA synthesis kit (Bio-Rad) and an oligo$(dT)_{20}$ primer on an Eppendorf Mastercycler (Eppendorf AG). Relative quantitation of transcript abundance was performed using an Eppendorf Mastercycler realplex2 (Eppendorf AG) and iQ SYBR Green supermix (Bio-Rad) using manufacturer's directions. All genotypes were quantified as averages of triplicate replicates and compared to *Rp49* amplification using Microsoft Excel and Prism (GraphPad).

2.6. Luciferase assays

S2 cells were transfected using relevant constructs containing the *act5c* or HSP70 promoter as well as the pNL3.1-VgQ reporter and pGL4.54 control. Induction of the HSP70 promoter was performed as described previously. Activation of the VgQ enhancer was monitored using the Nano-Glo Dual Luciferase Assay Kit (Promega) in 96-well plate format. Luminescence was measured on a BioTek Synergy2 plate reader. Analysis was performed using Excel (Microsoft) and Prism (Graphpad).

2.7. Fluorescence microscopy

Wing imaginal discs were dissected and stained with various antibodies as described previously (Hughes and Krause, 1999). The following primary antibodies were used at the indicated concentrations: rat anti-HA (1:50; Roche); mouse anti-Cut (Deposited by Gerald M. Rubin and obtained from the Developmental Studies Hybridoma Bank, The University of Iowa, Department of Biological Sciences, Iowa City, IA, 1:20). *Drosophila* embryos were collected overnight, fixed using 4% paraformaldehyde, and stained with antibodies as previously described (Hughes and Krause, 1999). Primary antibodies include rat anti-myosin MAC-147 (1:1000; Abcam). Species specific Alexa488, Alexa568-, and Alexa 647-conjugated secondary antibodies (1:10 000; Abcam) were used to recognize the primary antibodies. Images were obtained using either a spinning disc confocal system (Ultraview ERS; PE Biosciences) and CS9100-50 camera (Hamamatsu) with an Axioimager M2 microscope (Carl Zeiss) 40x Plan Apochromat lens 1.3NA, using Volocity acquisition software (PE Biosciences) or a Zeiss 700 scanning confocal microscope (Carl Zeiss) Plan Apochromat lens 1.3NA. Figures were assembled using Photoshop CS5 (Adobe).

3. Results

3.1. Scalloped promotes Vg phosphorylation

When Vg is expressed in S2 cells, multiple isoforms are observed by western blot, with one at the expected molecular weight and one prominent slower migrating band (Fig. 1A). Co-expression of 3xHA-Vg with relatively moderate levels of Sd induces the appearance of a prominent third slower migrating band (Fig. 1A). When a cell lysate isolated from cells expressing both Vg and Sd is pre-treated with increasing amounts of λ-phosphatase there is a corresponding loss of these slowest migrating bands (Fig. 1B).

The only post-translational modification of Vg known previously was sumoylation (Takanaka and Courey, 2005). However, the presence phosphatase sensitive isoforms (Fig. 1B) shows that Vg is also phosphorylated. The same result was observed with untagged Vg, indicating phosphorylation is neither dependent upon, nor caused by, the presence of a 6xMYC or 3xHA epitope tag (data not shown). Since Vg is dependent on Sd for nuclear import (Halder et al., 1998; Simmonds et al., 1998), it is possible a kinase localized to the nucleus is responsible for Sd-dependent phosphorylation. However, a version of Vg where the SV40 nuclear localization sequence (NLS) was added to the N-terminal of Vg did not show the slowest migrating isoform (3) unless Sd was co-expressed (Fig. 1C Nls-Vg). As Vg functions via binding Sd (Simmonds et al., 1998; Halder et al., 1998) we then tested it this interaction was required for Vg phosphorylation. A fusion protein containing Vg and the Sd TEA domain (Vg::Sd) produced 3 isoforms in the presence or absence of Sd (Fig. 1C Vg::Sd). A truncated Vg missing the TDU domain necessary for Sd interaction (ΔSID) did not exhibit the third band with or without Sd co-expression (Fig. 1C VgΔSID), even if this complex is directed to the nucleus by addition of an NLS (Fig. 1C NLS-VgΔSID). Collectively, this indicates that there is a requirement for a physical interaction between Vg and Sd for Vg post-translational phosphorylation, and that an interaction between Vg and a likely kinase is promoted by Sd.

To confirm the effect of co-expression of Sd results upon modification of Vg, two-dimensional Western blots were performed on S2 cell lysates. 6xMYC-Vg produces three distinct isoforms with different isoelectric point but the same molecular mass (Fig. 2A). Cells transfected with either 6xMYC-Vg alone and treated with λ-phosphatase show a single isoform

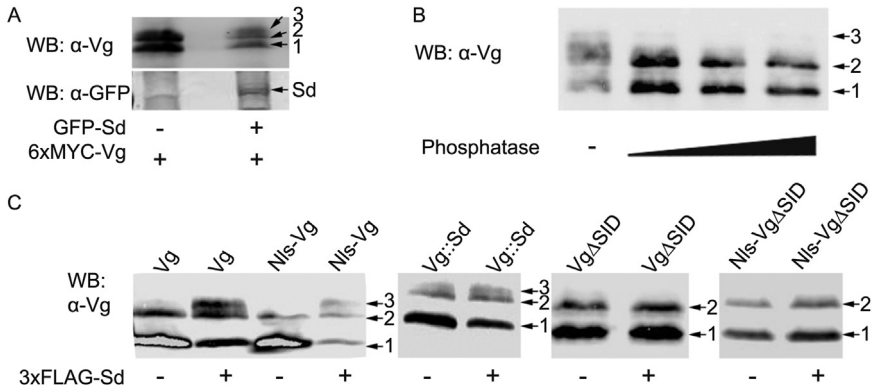

Fig. 1. Vestigial is post-translationally modified. A) Multiple isoforms of Vg (1–3) can be identified when separated in a low-bis polyacrylamide gel. S2 cells transfected with 6xMYC-Vg produce one faster running (baseline) Vg isoform (1) and a second slower isoform (2). When GFP-Sd is co-expressed, the relative proportion of isoforms 1 and 2 are altered and a relatively abundant additional slower migrating isoform (3) is seen. B) Pre-treatment of the S2 cell lysate with increasing concentrations of λ-phosphatase (indicated by the gradient below) shows a concomitant decrease in intensity of the second and third isoforms (2–3) indicating these are due to phosphorylation. C) Phospho-modification of Vg occurs in the nucleus and requires Sd. Wild type Vg and Vg fused to the SV40 nuclear localizing sequence (Nls), produce at least 3 at least three isoforms (1–3) in similar relative proportion when Sd is co-expressed (+). When transgenic fusions of full length Vg and Sd (Vg::Sd) are expressed, the requirement for Sd to form isoforms 2–3 is largely eliminated. A transgenic form of Vg deleted for the Scalloped interaction domain and as such, cannot bind Sd (VgΔSID) produces only the 1 and 2 isoforms with or with co-expression of Sd, even if the transgenic protein is directed to the nucleus Nls-VgΔSID. The arrows indicate isoforms represent fastest (1) to slowest migrating band (3).

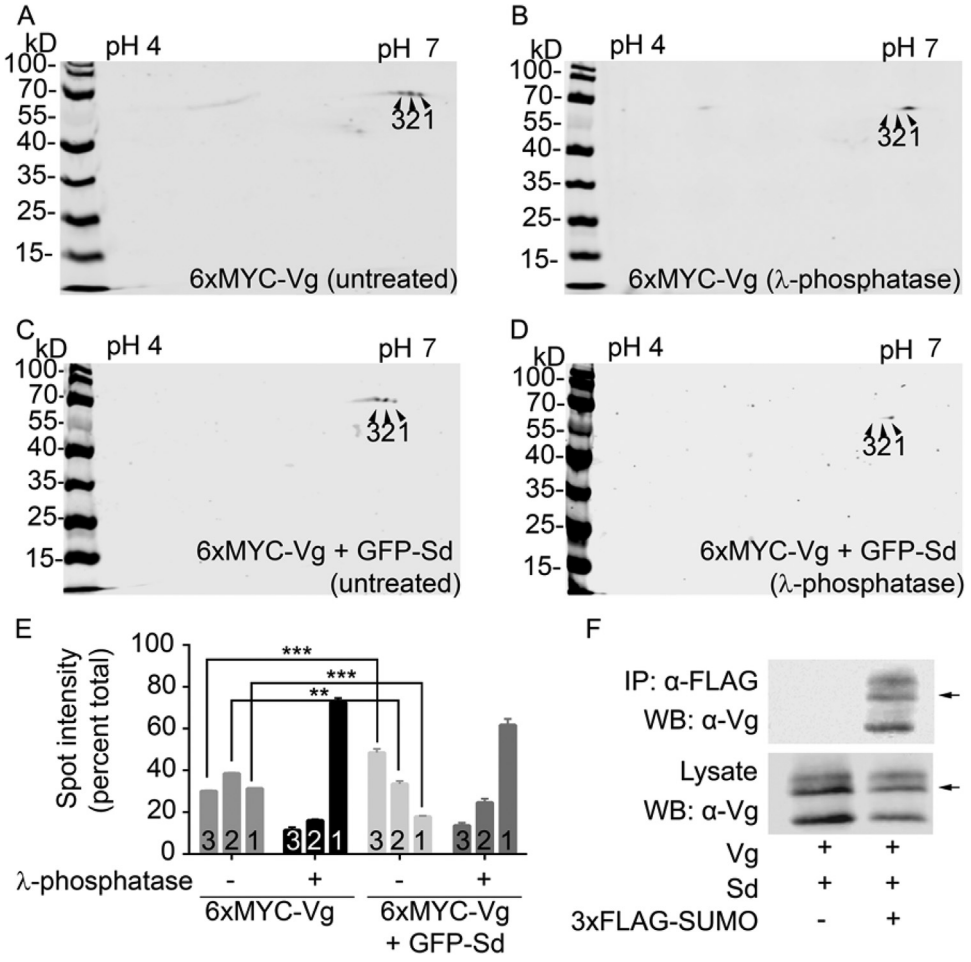

Fig. 2. Vg is preferentially phosphorylated in the presence of Sd. A) In an untreated lysate from cells expressing 6xMYC-Vg three isoforms of decreasing isoelectric point, are seen in approximately equal proportion. B) Pre-treatment of a lysate made from S2 cells expressing 6xMYC-Vg with λ-phosphatase produces three spots recognized by anti-Vg (1–3) with 1 being predominant. C) When 6xMYC-Vg and GFP-Sd are co-expressed spot 3 becomes even more predominant indicating that this is a phosphorylated form of Vg and that this modification is enhanced with increased expression of Sd. D) λ-phosphatase treated lysates from cells expressing 6xMYC-Vg and GFP-Sd also show a predominance of isoform 1. E) Quantification of the relative intensity of spots 1–3 in each condition. Values are averages of three independent experiments. Similar results (not shown) were also seen when an anti-MYC antibody was used (*** $p < 0.005$, ** $p < 0.01$). F) Immunoprecipitation of 3xFLAG-SUMO from cells co-transfected with Vg and Sd show that all three Vg isoforms are sumoylated equally.

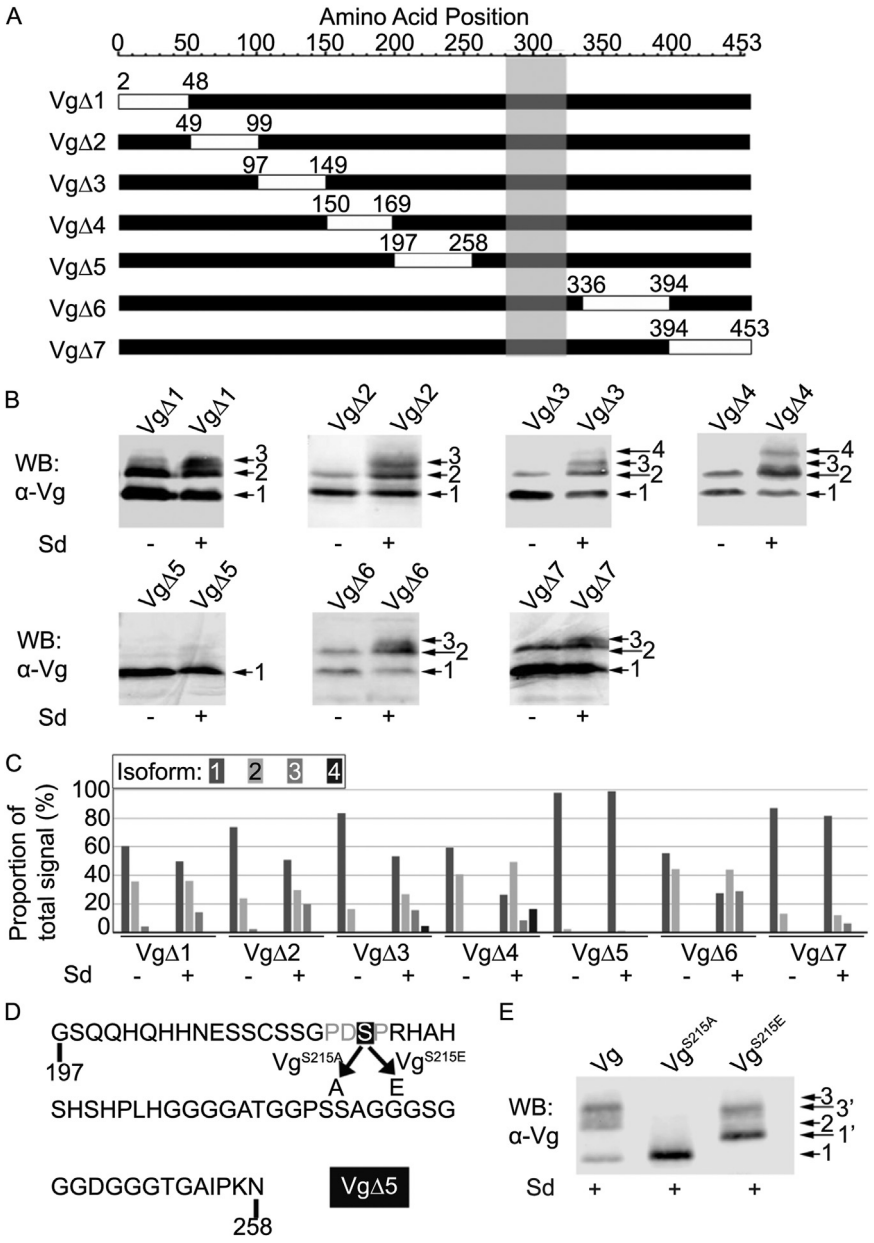

Fig. 3. Identification of the primary Vg phosphorylation site. A) A diagram showing a series of sequential deletions of Vg used for initial mapping of modified amino acids. The grey vertical bar represents the Sd interaction domain (SID)/TONDU domain. B) Paired western blot analysis of each of the Vg deletion constructs expressed in S2 cells. The presence/absence of slower migrating isoforms (1–4) are indicated for each. C) Relative quantification of each Vg isoform shown in B. Notably, VgΔ5 showed loss of all isoforms including the phosphatase resistant isoform 2 with and without Sd co-transfection. VgΔ7 showed proportionally less of phospho-isoform 3, while VgΔ3 and VgΔ4 lead to formation of even slower migrating Vg isoform 4. D) The amino acid sequence deleted in VgΔ5. A predicted MAPK phosphorylation site around Serine 215 was found within the VgΔ5 region. Transgenes of phosphomimetic (Vg^{S215E}) and non-phosphoryatable (Vg^{S215A}) mutations were created as indicated. E) Vg^{S215A} produces a single band the same size as seen with Vg at position 1. This is the same pattern of bands seen with VgΔ5. Notably, the phosphatase resistant band 2 is absent in Vg^{S215A}. Overexpression of phosphomimetic Vg^{S215E} consistently produced a unique banding pattern not previously observed. The band at position 1 is no longer seen, and the predominant band (1') is unique position compared to those seen with Vg or Vg^{S215A}. A slower running band is also observed with Vg^{S215E} (3') suggesting Vg^{S215E} is further modified.

the predicted size and isoelectric point of unmodified Vg (Fig. 2B). Co-transfection with GFP-Sd, causes an increase in the relative proportion of the most phosphorylated isoform (Fig. 2C). Again, these were confirmed to represent phosphorylated isoforms as λ-phosphatase treatment of lysates co-transfected with 6xMYC-Vg and GFP-Sd (Fig. 2D) leads to a shift toward the basal isoform (Fig. 2E). The same shift in isoform patterns was observed when membranes were probed with anti-Myc antibody (data not shown). Given that λ-phosphatase treatment reduced Vg to a single charge isoform, we tested Vg sumoylation (Takanaka and Courey, 2005) in similar lysates from cells co-expressing a 3xFLAG SUMO. Notably, we found that all Vg isoforms were sumoylated relatively equally (Fig. 2F).

3.2. Identification of Vestigial phosphorylation sites

Seven deletion mutants within Vg, (VgΔ1-VgΔ7) each removing approximately 50 amino acids, were generated to identify the general location of Vg modification sites (Fig. 3A). Western blotting of transfected S2 cell lysates indicated that only VgΔ5 showed a loss of all slower migrating isoforms (Fig. 3B-C). Within the VgΔ5 deleted sequence, there are 11 serine and 2 threonine and 1 lysine amino acids, with a consensus MAPK site at serine 215 (S215) (Fig. 3D). Mutagenesis of the potential phosphorylation sites within the VgΔ5 region to either a non-phosphorylatable amino acid (alanine, A) or one that mimics phosphorylated serine (glutamic acid, E) identified Ser215

as the key amino acid within the VgΔ5 region. Co-expression of the S215A and S215E Vg transgenes in S2 cells shows that the S215A mutation blocks all further Vg modification while the S215E phosphomimic showed enhanced post-translational modification (Fig. 3E).

3.3. Phosphorylation at Vestigial S215 affects wing development

To investigate whether S215 phosphorylation affects Vg function, we developed transgenic *Drosophila* expressing either a 3xHA-Vg^{S215A} or 3xHA-Vg^{S215E} transgene under the control of the UAS promoter. These transgenes were expressed using a synthetic GAL4 driver that contains two Vg enhancer elements, the quadrant enhancer (QE) and margin enhancer (ME). This repopulates the majority of the *vg* expression pattern in the wing blade, with ME driving expression along the wing imaginal disc dorsal/ventral boundary during the third larval instar and QE driving expression in the wing pouch. During larval development, these enhancers are self-activated by Vg in a feed-forward loop to delineate wing fate across the entire blade region of the wing disc (Kim et al., 1996; Williams et al., 1994).

Expression of Vg^{S215A} and Vg^{S215E} in a w^{1118} background produced no observable phenotypic effects (data not shown) producing wings indistinguishable from wild type (Fig. 4A), indicating that loss of phosphorylation does not have a dominant-negative effect on Vg function. Homozygous vg^{null} alleles are largely pupal lethal, with only a few adult escapers seen. These adults have extremely reduced wing imaginal discs and only vestigial wings suggesting a defect in proliferation, differentiation or likely both (Delanoue et al., 2004). The homozygous vg^{null} phenotype can be rescued by transgenic expression of Vg using the combined ME and QE Vg(M+Q) GAL 4 driver, although the overall wing size is often smaller (Fig. 4B). Expression of the 3xHA-Vg^{S215A} transgene in a homozygous vg^{null} background using *vg*(M+Q)-GAL4 partially rescues the vg^{null} wings-absent phenotype (Fig. 4C). However, clipping of the lateral wing margin reminiscent of a weak *vg* or *sd* loss of function was observed (Williams et al., 1991; Campbell et al., 1992). There was also a loss of sensory bristles along the anterior margin of the wing. This included instead showed a finer bristle structure reminiscent of the posterior wing margin (Fig. 4C'). Conversely, expression of the 3xHA-Vg^{S215E} transgene *vg*(M+Q)-GAL4 in a vg^{null} background largely restored both the wing blade and the differentiation of cells along the margin (Fig. 4D). However, in several instances a duplication of posterior margin sensory bristles (Fig. 4D') was observed. To ensure the observed differences were not due to variation between expression of each transgene, wing discs from the indicated genotypes were confirmed to have approximately equal *vg* expression via QRT-PCR (Fig. 4E). Similarly, the functional differences seen in wing specification caused by phosphomimicry at S215 are not simply due to the previously shown differential self-regulation of the *vg* QE enhancer (Halder and Carroll, 2001). A dual luciferase assay based on a reporter derived from the *vg*QE (Fig. 4F) showed that while co-expression of wild type Vg and Sd together could activate the QE significantly more than Vg alone, the activation of vgQE was far more muted when expressing the Vg^{S215A} nor Vg^{S215E} isoforms in S2 cells.

Sensory bristles in the adult wing are derived from sensory organ precursor (SOP) cells, located along the dorsal-ventral margin of the third instar wing disc. Subsets of these cells can be identified by expression of proneural genes like Cut (Ct) (Skeath and Carroll, 1991). Specification of wing margin SOPs requires Sd (Morcillo et al., 1996; Srivastava and Bell, 2003), but there is as yet no identified role for Vg in this process. To look more closely at SOP cell specification, third instar wing imaginal discs were examined for the pattern of cells expressing Ct along the presumptive dorsal-ventral wing margin. In a wild type wing disc, Ct positive cells can be seen in a narrow row along the dorsal/ventral boundary of the wing pouch (Fig. 5A, arrow). In homozygous vg^{null} larvae the wing discs, especially cells within the wing pouch region are largely absent and no Ct positive cells are present (data not shown). If a wild type *vg* transgene is expressed in a homozygous vg^{null} background, the wing disc is restored, although often at a reduced size, and Ct positive cells are seen along the dorsal-ventral margin of the wing pouch (Fig. 5B). When a 3xHA-Vg^{S215A} transgene is expressed in a vg^{null} background, the wing disc restored but only a few Ct positive cells are seen. (Fig. 5C α-Cut, arrow). This lack of Ct positive cells in the wing pouch is consistent with the adult wing loss of anterior margin SOP cells (Fig. 4B). Also, the pattern of cells expressing 3xHA-Vg^{S215A} is different than that seen with other transgenes expressed from the same *vg*(M+Q)-GAL4 driver. Cells immediately along the dorsal-ventral margin are not Vg-positive (Fig. 5C α-HA(Vg), arrow). When 3xHA-Vg^{S215E} is expressed in a vg^{null} background, the number and pattern of Ct positive cells is largely normal in comparison to the wild type wing disc, although there are some ectopic Ct positive cells and occasionally there are small gaps in the normal pattern of Ct-expressing cells along the dorsal-ventral border (Fig. 5D α-Cut, arrows). Note that each transgene was shown to have relatively equal *vg* mRNA expression (Fig. 4E). This suggests that phosphorylation at S215 is important for Vg induced differentiation of wing imaginal disc cells along the dorsal-ventral margin and maintenance of the vg margin enhancer (Halder et al., 1998), but not the Vg:Sd mediated proliferation of cells in the remainder of the wing disc mediated by the *vg*QE enhancer (Zecca and Struhl, 2007).

3.4. Embryonic muscle specification also requires Vg phosphorylation

We next examined the role of VgS215 modification in terms of embryonic muscle specification. We expressed the 3xHA-Vg^{S215A} and 3xHA-Vg^{S215E} transgenes under the control of a muscle-specific Mef2-GAL4 driver in a homozygous vg^{null} background to determine whether or not the phosphomimetic and non-phosphorylatable Vg isoforms were able to rescue the vg^{null} phenotype. The pattern of wild type somatic musculature has a repeated pattern of muscle-muscle and muscle-tendon attachments (Fig. 6A). Homozygous loss of Vg in the somatic musculature results in embryos with reduced viability, as well as muscle contraction defects and an incompletely penetrant loss of the VL2 muscle (Deng et al., 2009). Expressing 3xHA-Vg^{S215A} in homozygous vg^{null} embryos with was only able to partially rescue attachment phenotype in the VL muscles as there was still some rounding of the musculature indicative of weak attachments (Fig. 6B'). We also saw weak attachments in the ventral musculature (Fig. 6B''). Notably, this phenotype is similar to that observed in a *rhea*-sensitized, vg^{null} embryo (Deng et al., 2010). When the 3xHA-Vg^{S215E} transgene was expressed in the somatic musculature of a vg^{null} embryo, the resulting pattern of muscle attachments closely resembles wild type (Fig. 6C-C''). This indicates that the non-phosphorylated isoform of Vg is required for late stage muscle differentiation.

3.5. p38b is required for Vestigial phosphorylation

Within VgΔ5 region (Fig. 3D) is the MAPK consensus sequence Pro-Asp-Ser-Pro (Davis, 1993). The kinase prediction software GPS (Xue et al., 2011) also indicated that Serine 215 was a possible target of the p38 MAPK pathway. To test whether the p38b MAPK is responsible for phosphorylation of Vg, S2 cells transfected with 3xHA-Vg and 3xFLAG-Sd were treated with the pan-p38 MAPK inhibitor SB203580 (Han et al., 1998). Phosphorylation of Vg was diminished in a dose-dependent manner (Fig. 7A). A direct role of p38b Sd-dependent phosphorylation of Vg is supported by the observation that Sd and p38b co-immunoprecipitate (Fig. 7B).

MAPK proteins interact with targets through a docking (D) domain with the consensus sequence $(R/K)_{2-3}$-X_{1-6}-Φ_A-X-Φ_B, where Φ_A and Φ_B are hydrophobic residues (Jacobs et al., 1999). Within the TEA domain of Sd there are two of these motifs (Fig. 8A). This motif is not found in Vg. Deletion mutants of Sd missing sections of the TEA domain were examined for their effect on Vg phosphorylation. Deletion of either SdΔ1 or SdΔ2 showed loss of the slowest migrating Vg band with both

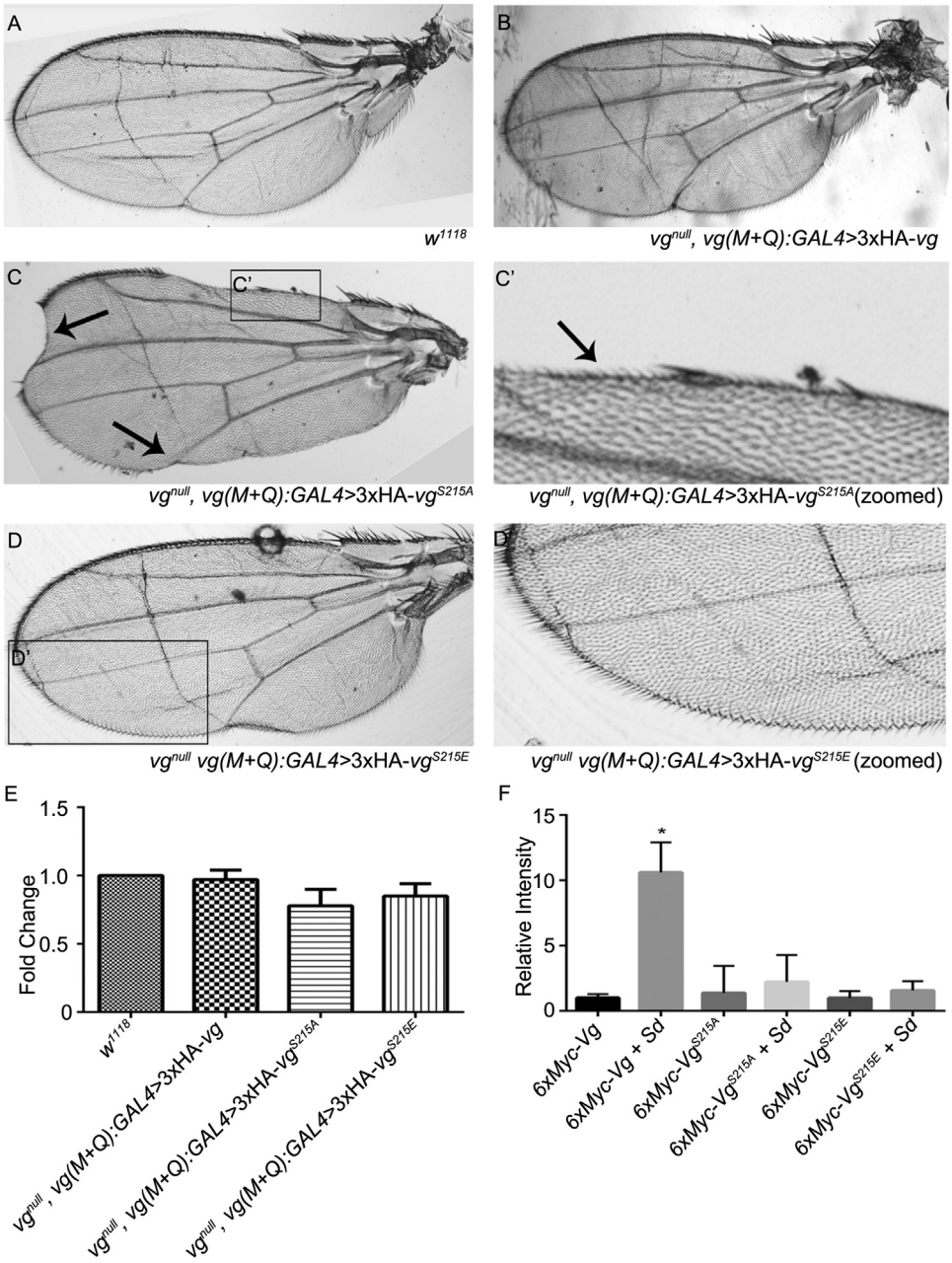

Fig. 4. Phosphorylation at S215 affects rescue of the wing development of a vg^{null} mutation by a *vg* transgene. A) A wild type wing showing the normal pattern of bristles at the anterior and posterior margins. B) Homozygous vg^{null} flies have no wings. Expressing UAS-3xHA-Vg under the control of a combined *vg* ME and QE driver - *vg*(M+Q)-GAL4 leads to a restoration of the adult wing including the margins. C) Similar expression of a 3xHA-Vg^{S215A} transgene only partially rescues the homozygous vg^{null} phenotype. The resulting adult wing shows clipping of the lateral margin and loss of anterior margin sensory bristles (in C' inset). D) Expressing the 3xHA-Vg^{S215E} transgene in a homozygous vg^{null} background produces a full size wing although aberrant differentiation of the posterior margin bristles is often seen(in D' inset). E) Quantitative RT-PCR measurement of mRNA isolated from dissected wing discs of the genotypes shown in A-D shows that the UAS-Vg, UAS-Vg^{S215A} and UAS-Vg^{S215E} transgenes are expressed at similar levels. F) Activation of the Vg QE by Vg, Vg^{S215A} and Vg^{S215E} with and without co-expression of Sd in S2 cells.

3xHA-Vg and 3xHA-Vg-NLS in S2 cells (Fig. 8B). To determine if one of the MAPK motifs was preferred, the consensus D domains were mutated with Arg-Lys replaced by Ala-Ala at position 145–146 ($Sd^{RK145AA}$) or Ser-Asn at positions 158–159 ($Sd^{RK158SN}$) and Ile-Gln with Ala-Ala at positions 152–153 ($Sd^{IQ152AA}$). Only $Sd^{RK158SN}$ caused a noticeable decrease in the level of Vg phosphorylation, as indicated by a decrease in intensity of the slowest migrating Vg band (Fig. 8C).

4. Discussion

Vg is a primary selector for wing fate in the developing *Drosophila* larva, and as such its regulation would need to be tightly controlled. Post-translational modifications such as phosphorylation have been shown with a variety of other proteins to provide a fine-tuned level of control over activity and expression (Lomelí and Vázquez, 2011; Talamillo et al., 2008; Tootle and Rebay, 2005). We have shown that phosphorylation plays important and different roles in regulating the activity of Vg during larval wing and embryonic muscle development. Notably, we found that phosphorylation of Vg is dependent on the presence of Sd, and alterations to the endogenous phosphorylation state of Vg can cause fate changes in the wing imaginal disc and somatic musculature.

Deletion of the VgΔ5 region (aa197-258) blocked post-translational phosphorylation of Vg (Fig. 3). Within this region, Serine 215 was

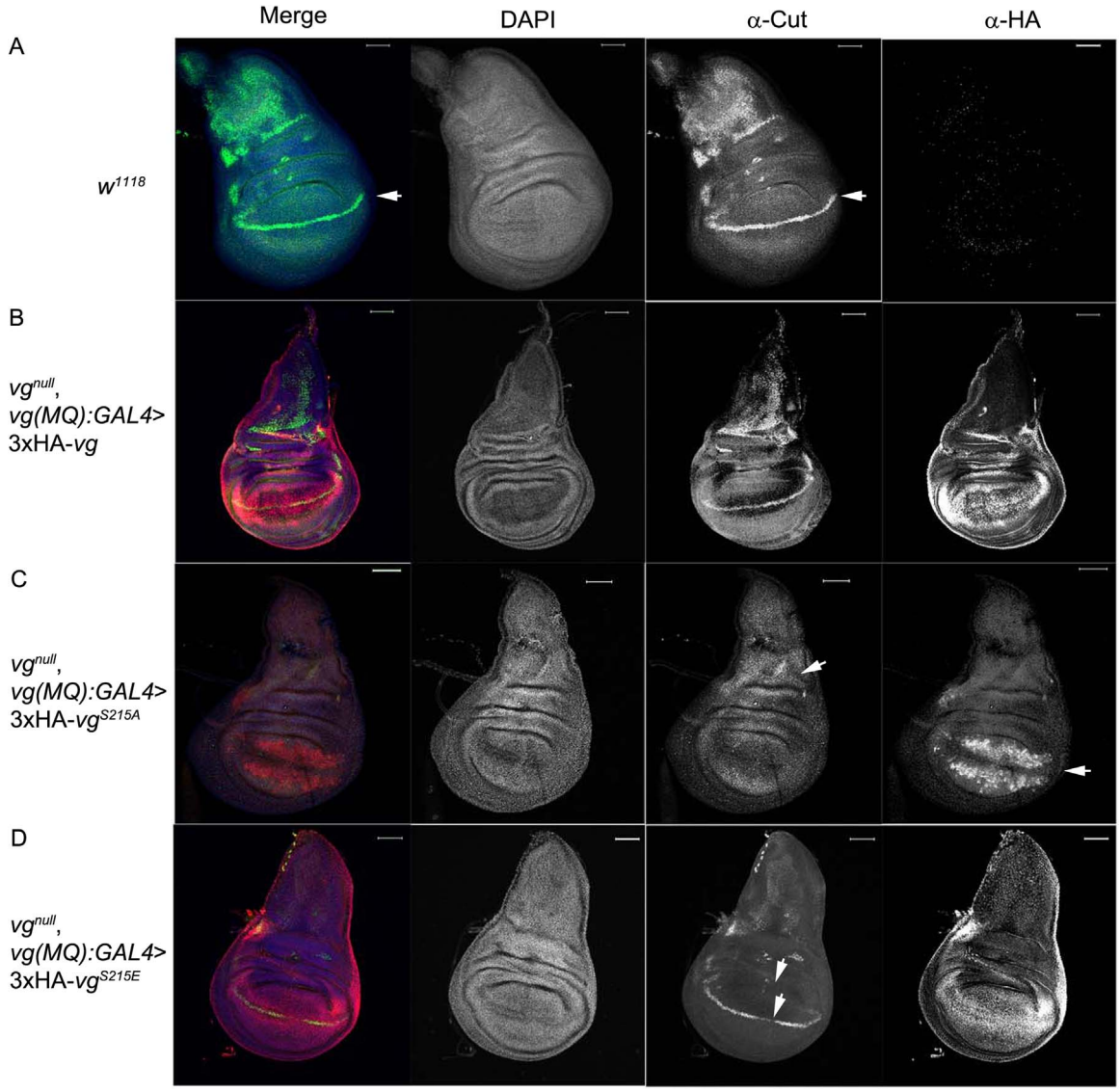

Fig. 5. Phosphorylation of Vg215 is necessary for wing imaginal disc growth and differentiation A) A wild type third instar larval wing disc showing normal expression of Cut (Ct). The row of Ct positive cells along the dorsal-ventral margin marks sensory organ precursors fated to become sensory bristles (arrow). B) Inducing expression of a 3xHA-Vg transgene along the wing margin via *vg*(M+Q)-GAL4 in a vg^{null} background produces a wing disc with reduced size compared to wild type but with a pattern of Ct expressing cells along the dorsal-ventral boundary that is similar to control wing discs. C) Similar expression of a 3xHA-Vg^{S215A} transgene in a vg^{null} background leads to a similar reduced size compared to wild type and few Ct positive cells (arrow), especially along the dorsal-ventral border. Also, the cells along the dorsal ventral margin do not express HA- Vg^{S215A} (arrow) D) Expression of a 3xHA-Vg^{S215E} transgene in a vg^{null} background largely restores the overall size of the wing disc and the pattern of Ct positive cells is similar to wild type. However some cells along the dorsal-ventral border do not express Ct and some ectopic Ct positive cells are seen adjacent to this region (arrows). Scale bar indicates 50 μm.

identified as the primary phosphorylation site on Vg. Modification of Vg^{S215} to the non-phosphorylatable alanine caused a loss of slower migrating bands indicating that subsequent phosphorylation events were dependent on S215 modification. This calls into question the role of other Vg modifications. Within the same VgΔ5 deletion there is also a lysine residue at position 257 (Fig. 3D). Sumoylation of Vg was previously established by Takanaka and Courey (2005) along with a functional relevancy for Vg sumoylation by Ubc9 in activating the *vg*QE. However, phosphatase pre-treatment of Vg lysates induces a single Vg isoform (Fig. 2). Similarly, deletion of the VgΔ5 results in form of Vg that is not post-translationally modified (Fig. 3). It appears that while Vg is sumoylated that each phospho-isoform is sumoylated equally. Within the VgΔ5 region, the single lysine K257 (Fig. 3D) was assayed as a potential target for SUMO conjugation. However, mutagenesis of K257 to arginine (Vg^{K257R}) did not result in measurable loss of sumoylation (not shown). This indicates that K257 is likely not a primary site for SUMO linkage, nor does the K257R mutation affect phosphorylation of Vg at S215. While sumoylation has been shown previously to be necessary for activation of the *vg*QE, there was no sensory bristle phenotype apparent in mutants for the sumoylation pathway in wings (Takanaka and Courey, 2005). Conversely, phosphomimicry at S215 was necessary for a rescuing effect of transgenic expressed Vg in terms of both restoration of the wing blade (proliferation) and sensory bristles at the wing margin (Figs. 4 and 5). It was also found that changes in the level of Vg itself, through expression of RNAi targeting Vg mRNA or a Vg overexpression construct, also do not show a sensory bristle phenotype in the wing (Baena-Lopez and García-Bellido, 2006). This is evidence that the phosphorylation of Vg, more so than sumoylation of Vg or titration of Vg protein levels, is responsible for directing fate change in a limited subpopulation of cells. Notably, addition of a SUMO modifier to a target protein would cause a basic shift in the pI, resolvable by 2-dimensional gel electrophoresis. In our experiments, pre-treatment of cell lysate transfected with 6xMyc-Vg using λ-phosphatase reduced the observable Vg to a single isoform (Fig. 2). This would indicate that all isoforms are phosphorylated and sumoylated, as there is no separate second point indicating a non-

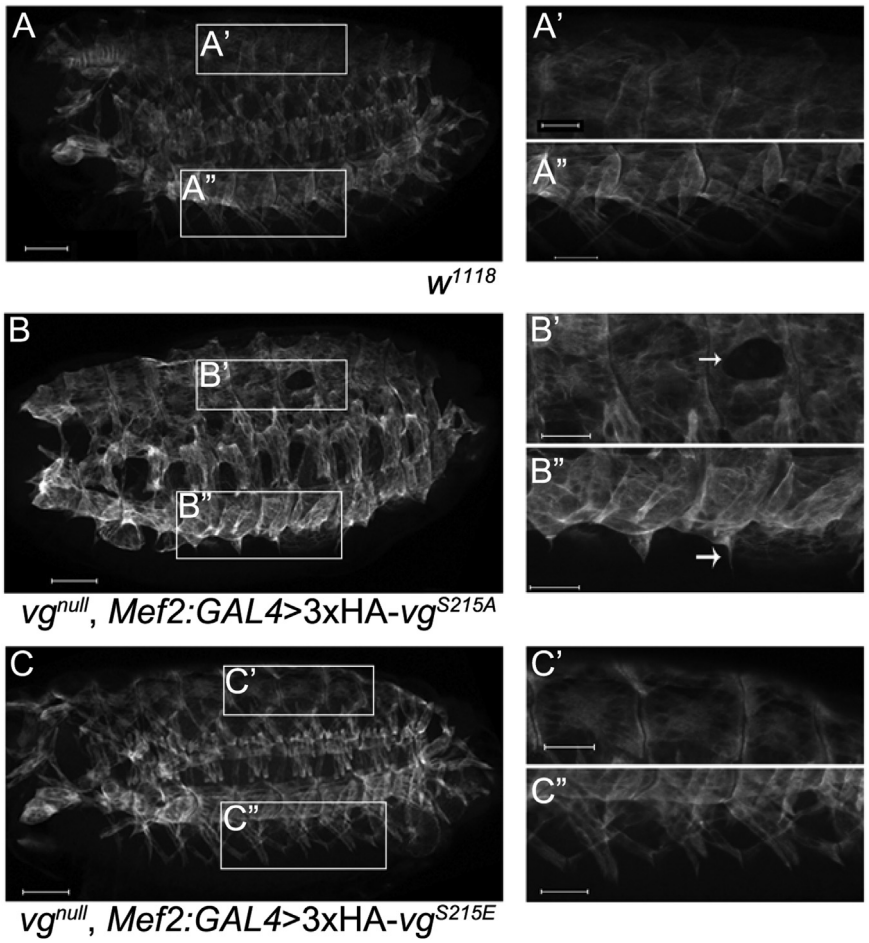

Fig. 6. Vestigial phosphorylation at Ser215 is required for late-stage muscle differentiation in embryos. A) An example of the pattern of somatic muscles in a wild type embryo. Close-up views of dorsal and ventral muscles are shown in A' and A" respectively. B) Expression of 3xHA-Vg^{S215A} in a homozygous *vg*^{null} embryo leads to poorly positioned muscle attachments at both the dorsal (B') and ventral (B") regions evidenced by irregular holes in the normal pattern of dorsal somatic muscles and muscles projecting into the ventral space (arrows). C) Expression of 3xHA-Vg^{S215E} can largely replace Vg function in terms of directing muscle attachment in a *vg*^{null} embryo. The attachment points and positioning of the dorsal (C') and ventral C") muscles are largely indistinguishable from wild type. Images shows are maximum projections with whole embryo scale bars of 40 μm and zoom scale bars of 20 μm.

sumoylated form of Vg showing an acidic shift. Together with the observation that all phospho-isoforms of Vg are sumoylated (Fig. 2F) this indicates that Vg sumoylation does not appear to have an impact on phosphorylation of Vg nor an effect in wing differentiation. However, the fact that both the Vg S215E and S215A isoforms were not able to significantly activate the *vg*QE enhancer (Fig. 4F) suggests that there are differential roles for each modificaiton. The interplay between phosphorylation and sumoylation is an avenue for further research, as it may potentially drive an even more refined ability to coordinate Vg function by permitting the protein to remain in a "poised" state ready for rapid activation or deactivation as development and fate specification progresses.

In vivo, there are differential phenotypic consequences to mimicking or blocking Vg phosphorylation at Ser 215. The weak rescue in of anterior margin sensory bristles in the vg^{null};*vg*(QM)-GAL4::UAS-*vg*^{S215A} flies (Fig. 4C) is indicative of a role for Vg phosphorylation in fate determination of SOPs, and the lateral margin wing clipping could be the result of a proliferation defect. Conversely, the pseudo-phosphorylated Vg^{S215E}-rescued wings have relatively good rescue of their anterior margins (Fig. 4D) with some posterior bristle duplication, and this Vg isoform is extensively phosphorylated in S2 cells in comparison to the wild type Vg construct (Fig. 3E). This phenotype may be due to an inability of the Vg^{S215A} mutant to sustain expression from the *vg*ME (Fig. 5C), suggesting a mechanism of differential control over developmental enhancers necessary for proper formation of the adult wing disc. The *vg*ME is active along the dorsal-ventral boundary of the wing

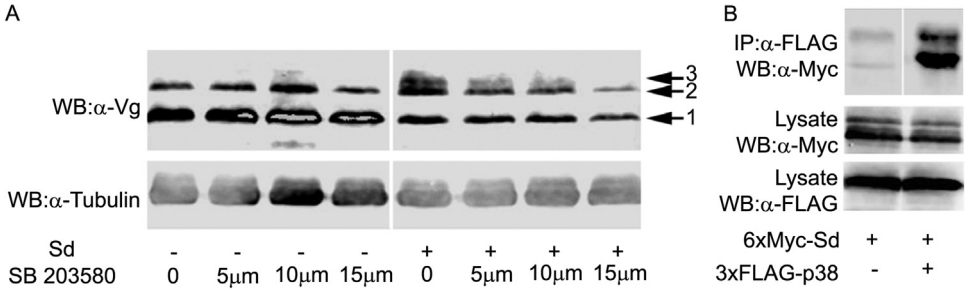

Fig. 7. p38 kinase is bound by Sd and inhibition of p38 reduces Sd induced Vg phosphorylation. A) S2 cell lysates co-transfected with Vg and Sd and treated with the pan-p38 MAPK inhibitor SB 203580 show a dose-dependent decrease in intensity of the phosphatase sensitive Vg band 3. B) 6xMYC-Sd is able to co-immunoprecipitate 3xFLAG-p38b.

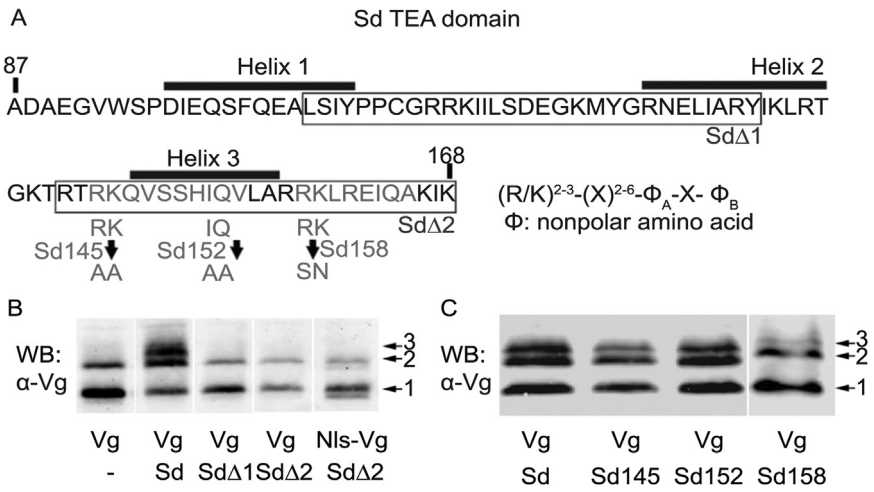

Fig. 8. The second MAPK motif within the Sd TEA domain is preferentially required for Vg phosphorylation. A) Schematic of Sd TEA domain deletions (SdΔ1 SdΔ2 - boxes) and mutations in MAPK D domains (Sd145, Sd152, Sd158; grey). B) Western blot analysis of S2 lysates co-transfected with 3xHA-Vg and Sd mutants show that the SdΔ1 and SdΔ2 deletions within the TEA domain of Sd block one but not both slower migrating bands from forming. C) Mutation of RK or IQ at Sd 145 and 152 did not lead to an alteration in the pattern of Vg isoforms 1–3. Mutation of RK at Sd^{158} caused a decreased intensity of the slowest migrating Vg band 3.

imaginal disc (Williams et al., 1994), whereas the remainder of the wing pouch is covered by the quadrant enhancer (Kim et al., 1996); a third enhancer, called the priming enhancer, provides a basal low level of Vg expression across the wing disc that permits future non-autonomous feed-forward regulation for the ME and QE enhancers (Zecca and Struhl, 2007). Rescue of the vg^{null} phenotype via expression of a wild type vg transgene fully restores the adult wing. However, the Vg^{S215A} transgene shows both a proliferative defect in the clipping of the lateral wing margin as well as a fate determination defect in the loss of the anterior sensory bristles. In the third instar wing disc, the Vg^{S215A} transgene only appears capable of sustaining the QE and not the ME. This can be compared to the Vg^{S215E} rescue, where there is no proliferative defect evidenced by an intact lateral margin, but mis-specification of the wing bristles is still apparent along the posterior margin and in SOP cells of the third instar wing disc. De-coupling of ME and QE activation by alternative Vg phosphorylation states indicates a mechanism of control for temporal and positional enhancer auto-regulation that is more fine-grained than a simple on/off process. By restricting the feed-forward loop during development, prospective wing blade and SOP cells can be properly identified within their fields; by inhibiting this using a non-phosphorylatable Vg mutant, the disc develops both a proliferative and identity defect phenotype that can only be partially corrected for using a phosphomimetic mutant. This is supported by the rescuing ability of these transgenes in embryonic musculature (Fig. 6). In muscle, VgS215A causes additional defects in muscle attachment formation, over what is seen with the vg^{null} genotype (Fig. 6C).

In S2 cells, co-expression of wild type Vg and Sd was able to significantly activate a luciferase reporter compared to over expression of Vg alone (Fig. 4F). However, nether the Vg^{S215A} or the Vg^{S215E} isoform could significantly recapitulate the exhibited activation of the luciferase reporter when co-expressed with Sd (Fig. 4F). This contrasts with the general ability of both the Vg^{S215A} and Vg^{S215E} mutants to rescue the vg^{null} absence of adult wings in Fig. 5. This may indicate that the ability to modulate the phosphorylation status is necessary in S2 cells, where wing-specific proteins are generally not expressed at appreciable levels. If Vg requires a change in phosphorylation status to fully assemble an activating complex, expressing solely non-phosphorylatable or phosphomimetic forms of the protein could prevent that complex from forming. In wing discs where wing-specific factors are endogenously expressed, the complex may be able to form more readily based on stochastic nucleation of the activation complex or availability of bridging proteins not expressed in S2 cells.

We have identified p38b as the kinase most likely directly responsible for Vg phosphorylation (Fig. 7). Previous studies have proposed some degree of functional overlap between p38b and p38a (also known as Mpk2), as double knockout mutants show larval and pupal lethality with few escapers (Chen et al., 2010). Expression of a strong dominant negative form of p38b using a wing disc GAL4 driver results in clipping of the lateral margin and shortening of the L5 wing vein (Adachi-Yamada et al., 1999), a phenotype similar to that shown by rescue of the vg^{null} phenotype by the Vg^{S215A} mutant transgene (Fig. 4). RNAi-mediated knockdown of p38b or p38a alone did not show any specific wing phenotype (data not shown), the phenotype may result from a stronger knockdown than the RNAi lines could achieve or due to some functional redundancy between p38b and p38a.

We have shown that p38b interacts directly with the Sd TEAD (Fig. 8), supporting a model where Sd acts as both a transcriptional partner to Vg as well as acting as a scaffold to promote post-translational modification of Vg to further refine its function and/or activity. A protein interaction map of the p38 MAPK family has been performed in *Drosophila* S2 cells, but did not retrieve either Vg or Sd as potential interaction targets (Belozerov et al., 2012); this is not unexpected as neither Vg nor Sd are appreciably expressed natively in S2 cells. Recent evidence showed that the Hippo pathway is regulated in part by p38b phosphorylation of Ajuba and modulation of F-actin accumulation, resulting in alterations in Yki-mediated gene regulation of Diap1 (Huang et al., 2016). It is possible that p38 MAPK may then interact with or regulate further downstream components of the Hippo signaling pathway, including Sd, and remains an avenue for investigation subsequent to our findings.

Finally, we have also demonstrated that phosphorylation of Vg is important across multiple cellular contexts. Rescue of vg^{null} embryos via expression of $3xHA\text{-}Vg^{S215A}$ and $3xHA\text{-}Vg^{S215E}$ were able to suppress the vg^{null} phenotype to differing extents. The non-phosphorylatable Vg^{S215A} was only partially able to rescue the poor muscle attachment phenotype (Fig. 6B) and caused poorly positioned muscle attachments, while Vg^{S215E} was able to rescue the phenotype to nearly full extent (Fig. 6C). This shows that post-translational modification of Vg is important in multiple tissues, and provides evidence that blocking phosphorylation of Vg at S215 attenuates full function of the protein. Precisely how this occurs is still unclear, but the post-translational modifications presented here may represent a mechanism of modulating Vg function until the appropriate point in terminal muscle differentiation.

Funding

This work was supported by a CIHR bridge grant from the Women's and Children's Health Research Institute – supported by the Stollery Children's Hospital Foundation, Edmonton Alberta and a Discovery Grant #386086 from the Natural Sciences and Engineering Research Council of Canada.

Acknowledgements

We would like to thank Dr. John Bell and Dr. Adam Magico for critical reading of the manuscript. We also appreciate assistance from the laboratory of Dr. Sarah Hughes.

References

Adachi-Yamada, T., Nakamura, M., Irie, K., Tomoyasu, Y., Sano, Y., Mori, E., Goto, S., Ueno, N., Nishida, Y., Matsumoto, K., 1999. p38 mitogen-activated protein kinase can be involved in transforming growth factor beta superfamily signal transduction in Drosophila wing morphogenesis. Mol. Cell Biol. 19, 2322–2329.

Alaggio, R., Zhang, L., Sung, Y.-S., Huang, S.-C., Chen, C.-L., Bisogno, G., Zin, A., Agaram, N.P., LaQuaglia, M.P., Wexler, L.H., Antonescu, C.R., 2015. A molecular study of pediatric spindle and sclerosing rhabdomyosarcoma: identification of novel and recurrent VGLL2-related fusions in infantile cases. Am. J. Surg. Pathol. 40, 224–235.

Baena-Lopez, L.A., García-Bellido, A., 2006. Control of growth and positional information by the graded Vestigial expression pattern in the wing of Drosophila melanogaster. Proc. Natl. Acad. Sci. USA 103, 13734–13739.

Belozerov, V.E., Lin, Z.-Y., Gingras, A.-C., McDermott, J.C., Siu, K.W.M., 2012. High resolution protein interaction map of the Drosophila melanogaster p38 mitogen-activated protein kinases reveals limited functional redundancy. Mol. Cell. Biol. 32, 3695–3706.

Bernard, F., Kasherov, P., Grenetier, S., Dutriaux, A., Zider, A., Silber, J., Lalouette, A., 2009. Integration of differentiation signals during indirect flight muscle formation by a novel enhancer of Drosophila vestigial gene. Dev. Biol. 332, 258–272.

Bernard, F., Lalouette, A., Gullaud, M., Jeantet, A.Y., Cossard, R., Zider, A., Ferveur, J.F., Silber, J., 2003. Control of apterous by vestigial drives indirect flight muscle development in Drosophila. Dev. Biol. 260, 391–403.

Campbell, S.D., Inamdar, M., Rodrigues, V., Raghavan, V., Palazzolo, M., Chovnick, A., 1992. The scalloped gene encodes a novel, evolutionarily conserved transcription factor required for sensory organ differentiation in Drosophila. Genes Dev. 6, 367–379.

Castilla, M.Á., López-García, M.Á., Atienza, M.R., Rosa-Rosa, J.M., Díaz-Martín, J., Pecero, M.L., Vieites, B., Romero-Pérez, L., Benítez, J., Calcabrini, A., Palacios, J., 2014. VGLL1 expression is associated with a triple-negative basal-like phenotype in breast cancer. Endocr. Relat. Cancer 21, 587–599.

Chen, H.-H., Maeda, T., Mullett, S.J., Stewart, A.F.R., 2004. Transcription cofactor Vgl-2 is required for skeletal muscle differentiation. Genesis 39, 273–279.

Chen, J., Xie, C., Tian, L., Hong, L., Wu, X., Han, J., 2010. Participation of the p38 pathway in Drosophila host defense against pathogenic bacteria and fungi. Proc. Nat. Acad. Sci. USA 107, 20774–20779.

Davis, R.J., 1993. The mitogen-activated protein kinase signal transduction pathway. J. Biol. Chem. 268, 14553–14556.

Delanoue, R., Legent, K., Godefroy, N., Flagiello, D., Dutriaux, A., Vaudin, P., Becker, J.L., Silber, J., 2004. The Drosophila wing differentiation factor Vestigial-Scalloped is required for cell proliferation and cell survival at the dorso-ventral boundary of the wing imaginal disc. Cell Death Differ. 11, 110–122.

Deng, H., Bell, J.B., Simmonds, A.J., 2010. Vestigial is required during late-stage muscle differentiation in Drosophila melanogaster embryos. Mol. Biol. Cell 21, 3304–3316.

Deng, H., Hughes, S.C., Bell, J.B., Simmonds, A.J., 2009. Alternative requirements for Vestigial, Scalloped, and Dmef2 during muscle differentiation in Drosophila melanogaster. Mol. Biol. Cell 20, 256–269.

Faucheux, C., Naye, F., Treguer, K., Fedou, S., Thiebaud, P., Theze, N., 2010. Vestigial like gene family expression in Xenopus: common and divergent features with other vertebrates. Int. J. Dev. Biol. 54, 1375–1382.

Gambaro, K., Quinn, M.C.J., Wojnarowicz, P.M., Arcand, S.L., de Ladurantaye, M., Barres, V., Ripeau, J.-S., Killary, A.M., Davis, E.C., Lavoie, J., Provencher, D.M., Mes-Masson, A.-M., Chevrette, M., Tonin, P.N., 2013. VGLL3 expression is associated with a tumor suppressor phenotype in epithelial ovarian cancer. Mol. Oncol. 7, 513–530.

Guss, K.A., Benson, M., Gubitosi, N., Brondell, K., Broadie, K.S., Skeath, J.B., 2013. Expression and function of scalloped during Drosophila development. Dev. Dyn. 242, 874–885.

Guss, K.A., Nelson, C.E., Hudson, A., Kraus, M.E., Carroll, S.B., 2001. Control of a genetic regulatory network by a selector gene. Science 292, 1164–1167.

Halder, G., Carroll, S.B., 2001. Binding of the Vestigial co-factor switches the DNA-target selectivity of the Scalloped selector protein. Development 128, 3295–3305.

Halder, G., Polaczyk, P., Kraus, M.E., Hudson, A., Kim, J., Laughon, A., Carroll, S.B., 1998. The Vestigial and Scalloped proteins act together to directly regulate wing-specific gene expression in Drosophila. Genes Dev. 12, 900–3909.

Han, Z.S., Enslen, H., Hu, X., Meng, X., Wu, I.-H., Barrett, T., Davis, R.J., Ip, Y.T., 1998. A conserved p38 mitogen-activated protein kinase pathway regulates Drosophila immunity gene expression. Mol. Cell Biol. 18, 3527–3539.

Han, K., 1996. An efficient DDAB-mediated transfection of Drosophila S2 cells. Nucleic Acids Res. 24, 4362–4363.

Hariharan, I.K., 2015. Organ size control: lessons from Drosophila. Dev. Cell 34, 255–265.

Huang, D., Li, X., Sun, L., Huang, P., Ying, H., Wang, H., Wu, J., Song, H., 2016. Regulation of Hippo signaling by p38 siganling. J. Mol. Cell Biol. 8, 328–337.

Hughes, S.C., Krause, H.M., 1999. Single and double FISH protocols for Drosophila. Methods Mol. Biol. 122, 93–101.

Jack, J., DeLotto, Y., 1992. Effect of wing scalloping mutations on cut expression and sense organ differentiation in the Drosophila wing margin. Genetics 131, 353–363.

Jacobs, D., Glossip, D., Xing, H., Muslin, A.J., Kornfeld, K., 1999. Multiple docking sites on substrate proteins form a modular system that mediates recognition by ERK MAP kinase. Genes Dev. 13, 163–175.

Jiang, W., Yao, F., He, J., Lv, B., Fang, W., Zhu, W., He, G., Chen, J., He, J., 2014. Downregulation of VGLL4 in the progression of esophageal squamous cell carcinoma. Tumour Biol. 36, 1289–1297.

Jiao, S., Wang, H., Shi, Z., Dong, A., Zhang, W., Song, X., He, F., Wang, Y., Zhang, Z., Wang, W., Wang, X., Guo, T., Li, P., Zhao, Y., Ji, H., Zhang, L., Zhou, Z., 2014. A peptide mimicking VGLL4 function acts as a YAP antagonist therapy against gastric cancer. Cancer Cell 25, 166–180.

Kim, J., Sebring, A., Esch, J.J., Kraus, M.E., Vorwerk, K., Magee, J., Carroll, S.B., 1996. Integration of positional signals and regulation of wing formation and identity by Drosophila vestigial gene. Nature 382, 133–138.

Koontz, L.M., Liu-Chittenden, Y., Yin, F., Zheng, Y., Yu, J., Huang, B., Chen, Q., Wu, S., Pan, D., 2013. The Hippo effector Yorkie controls normal tissue growth by antagonizing scalloped-mediated default repression. Dev. Cell 25, 388–401.

Laloux, I., Dubois, E., Dewerchin, M., Jacobs, E., 1990. TEC1, a gene involved in the activation of Ty1 and Ty1-mediated gene expression in Saccharomyces cerevisiae: cloning and molecular analysis. Mol. Cell Biol. 10, 3541–3550.

Li, H., Wang, Z., Zhang, W., Qian, K., Liao, G., Xu, W., Zhang, S., 2015a. VGLL4 inhibits EMT in part through suppressing Wnt/β-catenin signaling pathway in gastric cancer. Med. Oncol. 32, 83.

Li, N., Yu, N., Wang, J., Xi, H., Lu, W., Xu, H., Deng, M., Zheng, G., Liu, H., 2015b. miR-222/VGLL4/YAP-TEAD1 regulatory loop promotes proliferation and invasion of gastric cancer cells. Am. J. Cancer Res 5, 1158–1168.

Lomelí, H., Vázquez, M., 2011. Emerging roles of the SUMO pathway in development. Cell. Mol. Life Sci. 68, 4045–4064.

Maeda, T., Chapman, D.L., Stewart, A.F.R., 2002. Mammalian vestigial-like 2, a cofactor of TEF-1 and MEF2 transcription factors that promotes skeletal muscle differentiation. J. Biol. Chem. 277, 48889–48898.

Mann, C.J., Osborn, D.P.S., Hughes, S.M., 2007. Vestigial-like-2b (VITO-1b) and Tead-3a (Tef-5a) expression in zebrafish skeletal muscle, brain and notochord. Gene Expr. Patterns 7, 827–836.

Morcillo, P., Rosen, C., Dorsett, D., 1996. Genes regulating the remote wing margin enhancer in the Drosophila cut locus. Genetics 144, 1143–1154.

Paumard-Rigal, S., Zider, A., Vaudin, P., Silber, J., 1998. Specific interactions between vestigial and scalloped are required to promote wing tissue proliferation in Drosophila melanogaster. Dev. Genes Evol. 208, 440–446.

Peng, Z., Skoog, L., Hellborg, H., Jonstam, G., Wingmo, I.-L., Hjälm-Eriksson, M., Harmenberg, U., Cedermark, G.C., Andersson, K., Ährlund-Richter, L., Pramana, S., Pawitan, Y., Nistér, M., Nilsson, S., Li, C., 2014. An expression signature at diagnosis to estimate prostate cancer patients' overall survival. Prostate Cancer Prostatic Dis. 17, 81–90.

Pobbati, A.V., Hong, W., 2013. Emerging roles of TEAD transcription factors and its coactivators in cancers. Cancer Biol. Ther. 14, 390–398.

Sawada, A., Kiyonari, H., Ukita, K., Nishioka, N., Imuta, Y., Sasaki, H., 2008. Redundant roles of Tead1 and Tead2 in notochord development and the regulation of cell proliferation and survival. Mol. Cell Biol. 28, 3177–3189.

Sidor, C.M., Brain, R., Thompson, B.J., 2013. Mask proteins are cofactors of Yorkie/YAP in the Hippo pathway. Curr. Biol. 23, 223–228.

Simmonds, A.J., Liu, X., Soanes, K.H., Krause, H.M., Irvine, K.D., Bell, J.B., 1998. Molecular interactions between Vestigial and Scalloped promote wing formation in Drosophila. Genes Dev. 12, 3815–3820.

Simon E., Faucheux C., Zider A., Thézé N., Thiébaud P. From vestigial to vestigial-like: the Drosophila gene that has taken wing. Dev. Genes Evol. 226:297-315.

Skeath, J.B., Carroll, S.B., 1991. Regulation of achaete-scute gene expression and sensory organ pattern formation in the Drosophila wing. Genes Dev. 5, 984–995.

Srivastava, A., Mackay, J.O., Bell, J.B., 2002. A Vestigial: Scalloped TEA domain chimera rescues the wing phenotype of a *scalloped* mutation in *Drosophila melanogaster*. Genesis 33, 40–47.

Srivastava, A., Bell, J.B., 2003. Further developmental roles of the Vestigial/Scalloped transcription complex during wing development in Drosophila melanogaster. Mech. Dev. 120, 587–596.

Takanaka, Y., Courey, A.J., 2005. SUMO enhances Vestigial function during wing morphogenesis. Mech. Dev. 122, 1130–1137.

Talamillo, A., Sánchez, J., Barrio, R., 2008. Functional analysis of the SUMOylation pathway in Drosophila. Biochem. Soc. Trans. 36, 868–873.

Tootle, T.L., Rebay, I., 2005. Post-translational modifications influence transcription factor activity: a view from the ETS superfamily. Bioessays 27, 285–298.

Williams, J.A., Bell, J.B., 1988. Molecular organization of the vestigial region in Drosophila melanogaster. EMBO J. 7, 1355–1363.

Williams, J.A., Bell, J.B., Carroll, S.B., 1991. Control of Drosophila wing and haltere development by the nuclear vestigial gene product. Genes Dev. 5, 2481–2495.

Williams, J.A., Paddock, S.W., Vorwerk, K., Carroll, S.B., 1994. Organization of wing

formation and induction of a wing-patterning gene at the dorsal/ventral compartment boundary. Nature 368, 299–305.
Wu, S., Liu, Y., Zheng, Y., Dong, J., Pan, D., 2008. The TEAD/TEF family protein Scalloped mediates transcriptional output of the Hippo growth-regulatory pathway. Dev. Cell 14, 388–398.
Xue, Y., Liu, Z., Cao, J., Ma, Q., Gao, X., Wang, Q., Jin, C., Zhou, Y., Wen, L., Ren, J., 2011. GPS 2.1: enhanced prediction of kinase-specific phosphorylation sites with an algorithm of motif length selection. Protein Eng. Des. Sel. 24, 255–260.
Yagi, R., Kohn, M.J., Karavanova, I., Kaneko, K.J., Vullhorst, D., DePamphilis, M.L., Buonanno, A., 2007. Transcription factor TEAD4 specifies the trophectoderm lineage at the beginning of mammalian development. Development 134, 3827–3836.
Zecca, M., Struhl, G., 2007. Control of wing growth by the Drosophila quadrant enhancer. Development 134, 3011–3020.
Zhang, L., Ren, F., Zhang, Q., Chen, Y., Wang, B., Jiang, J., 2008. The TEAD/TEF family of transcription factor Scalloped mediates Hippo signaling in organ size control. Dev. Cell 14, 377–387.
Zhang, W., Gao, Y., Li, P., Shi, Z., Guo, T., Li, F., Han, X., Feng, Y., Zheng, C., Wang, Z., Li, F., Chen, H., Zhou, Z., Zhang, L., Ji, H., 2014. VGLL4 functions as a new tumor suppressor in lung cancer by negatively regulating the YAP-TEAD transcriptional complex. Cell Res. 24, 331–343.
Zhao, B., Li, L., Lei, Q., Guan, K.-L., 2010. The Hippo-YAP pathway in organ size control and tumorigenesis: an updated version. Genes Dev. 24, 862–874.